



Research and Development

Measurement of Fugitive Emissions at
a Region I Landfill

Prepared for

U.S. Environmental Protection Agency Region I

Prepared by

National Risk Management
Research Laboratory
Research Triangle Park, NC 27711

Measurement of Fugitive Emissions at a Region I Landfill

by

Mark Modrak, Ram Hashmonay, and Robert Keagan
ARCADIS Geraghty & Miller
P.O. Box 13109
Research Triangle Park, NC 27709

Contract No. 68-C99-201, Work Assignment No. 4-003

EPA Project Officer: Susan A. Thorneloe
Air Pollution Prevention and Control Division
National Risk Management Research Laboratory
Research Triangle Park, NC 27711

Prepared for:

U.S. Environmental Protection Agency
Office of Research and Development
Washington, DC 20460

Abstract

This report discusses a new measurement technology for characterizing emissions from large area sources. This work was funded by EPA's Monitoring and Measurement for the 21st Century Initiative, or 21M2. The site selected for demonstrating this technology is a superfund landfill that is being evaluated for recreational use. Data on methane and air toxics were needed to help determine any increased risk to those using the site. Open-path Fourier transform infrared (OP-FTIR) spectrometers were used to provide data on both background and surface emissions. The technology provides concentration maps indicating the spatial variability and areas where additional control may be needed. Horizontal scans to identify any hot spots and vertical scans to determine the mass flux using a multiple-beam configuration were conducted. Optical remote sensing-radial plume mapping provided concentration mapping of the site. These data will be used to make decisions about potential recreational use of this site.

Foreword

The U.S. Environmental Protection Agency (EPA) is charged by Congress with protecting the Nation's land, air, and water resources. Under a mandate of national environmental laws, the Agency strives to formulate and implement actions leading to a compatible balance between human activities and the ability of natural systems to support and nurture life. To meet this mandate, EPA's research program is providing data and technical support for solving environmental problems today and building a science knowledge base necessary to manage our ecological resources wisely, understand how pollutants affect our health, and prevent or reduce environmental risks in the future.

The National Risk Management Research Laboratory (NRMRL) is the Agency's center for investigation of technological and management approaches for preventing and reducing risks from pollution that threaten human health and the environment. The focus of the Laboratory's research program is on methods and their cost-effectiveness for prevention and control of pollution to air, land, water, and subsurface resources; protection of water quality in public water systems; remediation of contaminated sites, sediments and ground water; prevention and control of indoor air pollution; and restoration of ecosystems. NRMRL collaborates with both public and private sector partners to foster technologies that reduce the cost of compliance and to anticipate emerging problems. NRMRL's research provides solutions to environmental problems by developing and promoting technologies that protect and improve the environment; advancing scientific and engineering information to support regulatory and policy decisions; and providing the technical support and information transfer to ensure implementation of environmental regulations and strategies at the national, state, and community levels.

This publication has been produced as part of the Laboratory's strategic long-term research plan. It is published and made available by EPA's Office of Research and Development to assist the user community and to link researchers with their clients.

Lee A. Mulkey, Acting Director
National Risk Management Research Laboratory

EPA REVIEW NOTICE

This report has been peer and administratively reviewed by the U.S. Environmental Protection Agency and approved for publication. Mention of trade names or commercial products does not constitute endorsement or recommendation for use.

This document is available to the public through the National Technical Information Service, Springfield, Virginia 22161.

Contents

<u>Section</u>	<u>Page</u>
Abstract	ii
Foreword	iii
EPA Review Notice	iv
List of Figures	vii
List of Tables	viii
 Executive Summary	 E-1
E1. Background/Site Information	E-1
E1.1 Horizontal Radial Plume Mapping	E-2
E1.2 Vertical Radial Plume Mapping	E-2
E2. Results and Discussions	E-2
E2.1 Horizontal Radial Plume Mapping Results	E-2
E2.2 Vertical Radial Plume Mapping Results	E-3
E2.3 Hazardous Air Pollutants	E-4
E3. Concluding Statements	E-4
1.0 Introduction	1-1
1.1 Background	1-1
1.2 Project Purpose and Description	1-2
1.2.1 Horizontal Radial Plume Mapping	1-4
1.2.2 Vertical Radial Plume Mapping	1-5
1.3 Data Quality Objectives and Criteria	1-6
1.4 Schedule of Work Performed for Project	1-8
2.0 The Measurements	2-1
2.1 Area A	2-1
2.2 Area B	2-3
2.3 Area C	2-4
2.4 Area D	2-5
2.5 Area E	2-5
2.6 Vertical Scanning	2-7
2.7 Meteorological Data	2-7

Contents (continued)

<u>Section</u>	<u>Page</u>
2.8 Data Analysis	2-8
3.0 Analytical Results and Discussion	3-1
3.1 The Horizontal RPM Results	3-1
3.2 The Vertical RPM Results	3-9
3.3 The Search for HAPs and Other Chemicals	3-12
4.0 Quality Assurance/Quality Control	4-1
4.1 Assessment of DQI Goals	4-1
4.2 Ethylene Tracer Release	4-2
4.3 Assessment of Number of Cycles Used for Moving Average	4-5
5.0 Conclusion	5-1
6.0 References	6-1

List of Figures

<u>Figure</u>	<u>Page</u>
1-1 Map of the Somersworth Superfund Landfill	1-2
1-2 Overhead View of an Example Horizontal RPM Configuration	1-4
1-3 Example of a Vertical RPM Configuration	1-5
2-1 Schematic of OP-FTIR RPM Measurement Configuration in Area A	2-2
2-2 Schematic of OP-FTIR RPM Measurement Configuration in Area B	2-3
2-3 Schematic of OP-FTIR RPM Measurement Configuration in Area C	2-4
2-4 Schematic of OP-FTIR RPM Measurement Configuration in Area D	2-5
2-5 Schematic of OP-FTIR RPM Measurement Configuration in Area E	2-6
3-1 Reconstructed Methane Concentrations (in ppmv) for Area A	3-3
3-2 Reconstructed Methane Concentrations (in ppmv) for Area B	3-4
3-3 Reconstructed Methane Concentrations (in ppmv) for Area C	3-5
3-4 Reconstructed Methane Concentrations (in ppmv) for Area D	3-6
3-5 Reconstructed Methane Concentrations (in ppmv) for Area E	3-7
3-6 The OP-FTIR RPM Methane Concentration Contours Overlaid on the Map of the Somersworth Superfund Landfill.	3-8
3-7 Vertical Scan RPM Measurement of the Vertical Methane Plume Profile	3-10
3-8 Vertical Scan RPM Measurement of the Plume Profile from the Hot Spot in the Valley	3-11
3-9 Two Beam RPM Measurement of the Vertical Methane Plume Profile on the Western (Upwind) Side of the Landfill	3-12
4-1 OP-FTIR RPM Measurement of the Vertical Ethylene Tracer Plume Profile on the Western (Upwind) Side of the Landfill	4-3
4-2 Time Series of the Calculated Ethylene Flux from Tracer Release Experiment	4-5
4-3 Calculated Average Methane Flux and Average CCF from the Vertical Scanning Survey	4-6

List of Tables

<u>Table</u>	<u>Page</u>
E1. Range of Mean Methane Concentrations (in ppmv above global background) Found in Each Survey Area.	E-3
1-1 DQI Goals for Critical Measurements	1-6
1-2 Detection Limits for Target Compounds	1-7
1-3 Schedule of Work Performed for Somersworth, NH Field Study	1-9
2-1 Coordinates of Mirrors Used for Horizontal Scanning in Area A	2-2
2-2 Coordinates of Mirrors Used for Horizontal Scanning in Area B	2-3
2-3 Coordinates of Mirrors Used for Horizontal Scanning in Area C	2-4
2-4 Coordinates of Mirrors Used for Horizontal Scanning in Area D	2-6
2-5 Coordinates of Mirrors Used for Horizontal Scanning in Area E	2-7
2-6 Coordinates of Mirrors Used for Vertical Scanning	2-7
3-1 Moving Average of Calculated Methane Flux, CCF, Wind Speed, and Wind Direction for the Vertical Scanning Survey	3-2
3-2 Mean Methane Concentration (ppm) Determinations for Each Area	3-7

Executive Summary

E1. Background/Site Information

A field study was performed during September and October, 2002 by ARCADIS and the U.S. EPA to measure emissions from a superfund site in Somersworth, New Hampshire using an open-path Fourier transform infrared (OP-FTIR) spectrometer. The study involved a technique, developed through research funded by the EPA's National Risk Management Research Laboratory (NRMRL), which uses optical remote sensing-radial plume mapping (ORS-RPM) to evaluate fugitive emissions.

The focus of the study was to characterize the emissions of methane and hazardous air pollutants to assess landfill gas emissions from the site. The results will help determine whether active controls will be required at the site. Concentrations of each compound were measured, and fluxes (determined as the rate of flow per unit time, through a unit area) were calculated for each compound detected. The site was divided into five survey areas for the field campaign. Detailed maps of each survey area, and the survey configurations used in each area are included in the report (see Figures 1-1, 2-1 through 2-5, and Tables 2-1 through 2-5).

The ORS-RPM techniques used in the present study were designed to characterize the emissions of fugitive gases from area sources. Detailed spatial information is obtained from path-integrated ORS measurements by the use of optimization algorithms. The method involved the use of an innovative configuration of non-overlapping radial beam geometry to map the concentration distributions in a plane. This method, radial plume mapping (RPM) (Hashmonay et al., 1999; Wu et al., 1999; Hashmonay et al., 2002), can also be applied to a vertical plane downwind from an area emission source to map the crosswind and vertical profiles of a plume. By incorporating wind information, the flux through the plane is calculated, which leads to an emission rate of the upwind area source.

E1.1 Horizontal Radial Plume Mapping

Horizontal scanning was performed in each of the five survey areas (see Figure 1-1) to search for emission hot spots. Area A is located in the northwestern section of the landfill site; Area B is located in the southeastern section of the site and includes a baseball field and basketball courts; Area C is located in the northern section of the site and includes a baseball field; Area D is located inside the chain-link fence of four tennis courts in the northeastern corner of the site; Area E is located in the southwestern section of the site.

E1.2 Vertical Radial Plume Mapping

The vertical scan configuration was set up along the eastern boundary of the landfill site. This location was chosen because it was optimum for determining a flux that would be representative of the entire site under the given wind conditions. Figure 1-1 shows the location of the vertical scanning configuration (the red line shows the location of the vertical plane, the red dot shows the location of the OP-FTIR instrument, and the red square shows the location of the scissors jack).

E2. Results and Discussions

An emissions contour map of the entire site and identification of three emission hot spots was obtained from radial plume mapping. Vertical scanning enabled an estimate of the methane flux from the entire site to be made.

E2.1 Horizontal Radial Plume Mapping Results

Horizontal scans were performed at each of the five survey areas. Figures 3-1 through 3-5 show the average reconstructed methane concentrations in parts per million by volume for Areas A, B, C, D, and E, respectively. The global methane background value of 1.75 ppm was subtracted from each of the measurements taken. Table E1 shows a range of the area-averaged methane concentrations measured in the five areas.

Table E1. Range of Mean Methane Concentrations (in ppmv above global background) Found in Each Survey Area.

Area	Range of Methane Concentrations
A	0.00 to 2.69
B	0.56 to 1.83
C	0.00 to 3.06
D	0.00 to 1.91
E	0.00 to 1.44

The measured surface methane concentrations ranged from the global background to 3.06 ppm. The average methane concentration found was 1.03 ppm above global background.

Figure 3-6 shows the horizontal RPM-determined methane concentration contours overlaid on a map of the Somersworth site. The determination of this concentration map is based solely on the mean path-integrated measurements made in each survey area, and six auxiliary path-integrated measurements made by an additional OP-FTIR instrument. Figure 3-6 shows three methane hot spots, one in Area A (2.5 ppm above ambient), the second in the northwest corner of Area C (3.0 ppm above ambient), and the third hot spot, the most intense at 6.5 ppm above ambient, occurred in a small valley that lies north of the baseball field in Area B. This hot spot was identified in sub-area B, so the additional OP-FTIR instrument was set up in the valley and made six auxiliary measurements. These six measurements provided the detail showing the sharp concentration gradients shown in Figure 3-6. Strong methane emissions were located near an uncapped vent that was on the south slope of the valley adjacent to Area B.

E2.2 Vertical Radial Plume Mapping Results

Vertical scanning was done on the eastern boundary of the landfill to determine a methane flux from the entire site, which was estimated to be 5.8 g/s. Additionally, the methane flux from the hot spots (found during the surface scanning survey) was estimated by modifying the vertical scanning configuration slightly. The estimated methane flux from the hot spots was 3.3 g/s, which represents 57 percent of the emission from the entire landfill.

E2.3 Hazardous Air Pollutants

All data collected at the site, including data from horizontal and vertical scanning surveys, were analyzed for any chemicals that are normally not found in the atmosphere, and this analysis did not detect the presence of any of these chemicals at the site. This result is not surprising when one notes that the maximum methane concentration measured at the landfill was 6.5 ppm, and the minor constituents (neglecting aliphatic hydrocarbons) occur in landfills at levels that are typically much less than 10^{-4} times the methane levels. Thus, minor constituents of the landfill gases would be expected to be present at levels much lower than the detection limits of the OP-FTIR instrument.

E3. Concluding Statements

The present study employed OP-FTIR sensors to determine chemical concentrations over the entire area of the Superfund landfill in Somersworth, New Hampshire. The spatial information was extracted from path-integrated OP-FTIR measurements using the RPM method. This measurement-based technique provided a complete methane concentration-contour map of the entire landfill and located methane emission hot spots (up to 6.5 ppm average above the global background). In addition, the vertical scanning technique provided an estimate for the methane emission from the entire landfill of 5.8 g/s. The methane emission rate from the hot spots in the valley was determined to be 3.3 g/s, which is estimated to be 57 percent of the emission from the entire landfill.

1.0

Introduction

1.1 Background

A superfund site in Somersworth, New Hampshire is being considered for re-use as a soccer field/recreational area, and the state has requested a study to assess landfill gas emissions from this site. The results will help determine whether active controls will be required. The focus of the study was to characterize the emissions of methane and hazardous air pollutants. The study employed optical remote sensing (ORS) techniques to determine chemical concentrations over the entire area of the landfill. These techniques result in the generation of maps showing the locations of high methane concentrations. In addition, concentration contour lines (isopleths) were generated in the downwind vertical plane from which emission rates were determined.

There is much concern over the potential hazards of landfill gas emissions. Hazardous air pollutants (HAPs) at sufficient levels can result in negative health effects due to both short-term and long-term exposures. The predominant component of landfill emissions is methane, which can result in fire and possible explosions at high levels. Methane is also a major greenhouse gas that is implicated in global warming. Adding to these concerns is the annoyance of the odors due to some of the minor components of landfill gases. EPA has promulgated regulations under the Clean Air Act to address the public health and welfare concerns of landfill gas emissions. The final rule and guidelines are contained in 40 CFR Parts 51, 52, and 60, Standards of Performance for New Stationary Sources and Guidelines for Control of Existing Sources: Municipal Solid Waste Landfills.

The Somersworth site was divided into five rectangular survey areas (A-E). Figure 1-1 presents the overall layout of the Somersworth Superfund Site, detailing the geographic location of each survey region. Additionally, the figure shows the location of the vertical scanning configuration, which was used to gather data in order to calculate emission fluxes for the entire site.

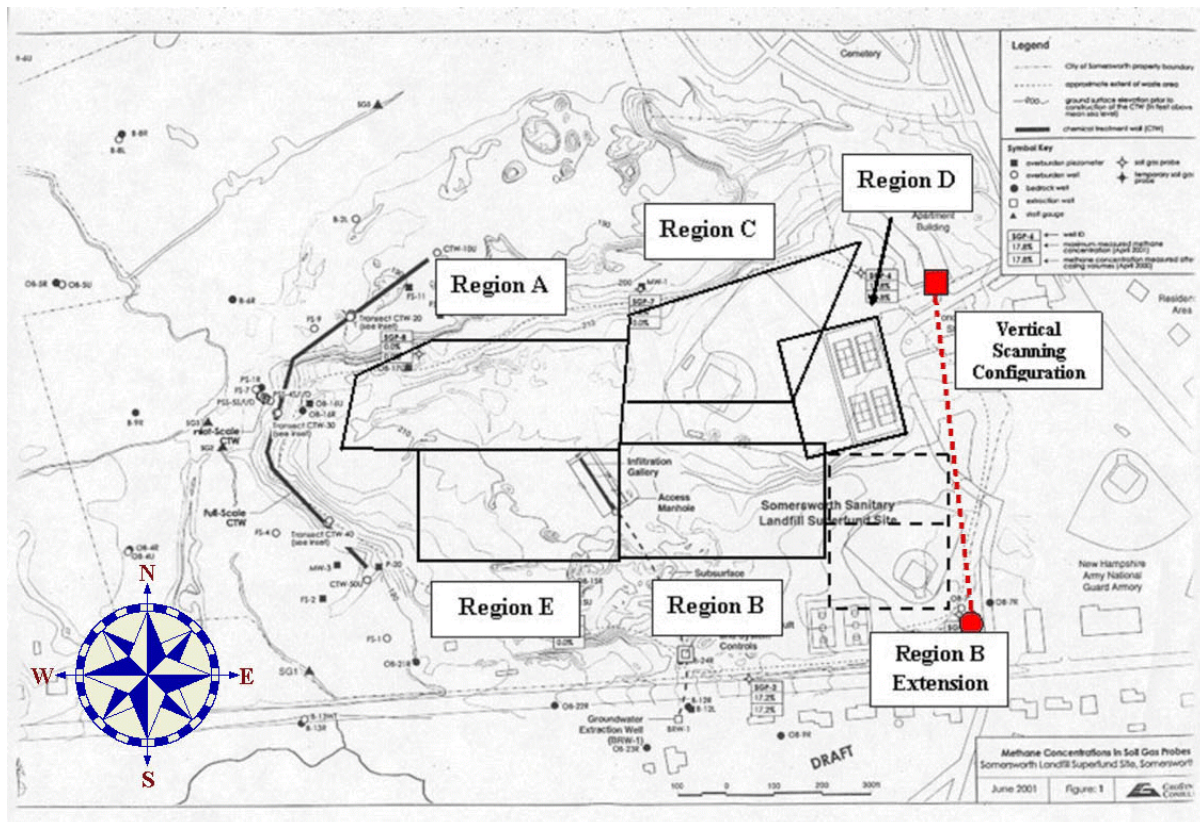


Figure 1-1. Map of the Somersworth Superfund Landfill

1.2 Project Purpose and Description

The optical remote sensing (ORS) techniques used in the present study were designed to characterize the emissions of fugitive gases from area sources. These techniques were developed in research and development programs funded by the U.S. EPA's National Risk Management Research Laboratory (NRMRL). Detailed spatial information is obtained from path-integrated ORS measurements by the use of optimization algorithms. The method involved the use of an innovative configuration of non-overlapping radial beam geometry to map the concentration distributions in a plane. This method, radial plume mapping (RPM) (Hashmonay et al., 1999; Wu et al., 1999; Hashmonay et al., 2002), can also be applied to a vertical plane downwind from an area emission source to map the crosswind and vertical profiles of a plume. By incorporating wind information, the flux through the plane is calculated, which leads to an emission rate of the upwind area source. An open-path Fourier transform infrared (OP-FTIR) sensor manufactured

by Unisearch Associates was chosen for the present study because of its capability of accurately measuring a large number of chemical species that might occur in a plume.

The OP-FTIR spectrometer combined with the RPM method can be used for both fence-line monitoring applications, and real-time, on-site, remediation monitoring and source characterization. An infrared light beam modulated by a Michelson interferometer is transmitted from a single OP-FTIR instrument to a corner cube mirror target, which is usually set up at a range of 100 to 500 meters. The returned light signal is received by the single telescope and directed to a detector. The light is absorbed by the molecules in the beam path as the light is transmitted to the mirror and again as the light is reflected back to the analyzer. Thus, the round-trip path of the light doubles the chemical absorption signal. The OP-FTIR measures the path-integrated concentration (PIC) along the beam path. One advantage of OP-FTIR monitoring is that the concentrations of a multitude of infrared absorbing gaseous chemicals can be detected and measured simultaneously with high temporal resolution.

The chemical vapor emitted from an emission source forms a plume, which is carried by the wind across the multiple infrared beams. The OP-FTIR PIC measurements can be used with wind data to calculate the emission rate applying the RPM method for vertical planes. The beam measurements avoid the uncertainties that are inherent in the traditional point measurements.

Meteorological and survey measurements were also made. A theodolite was used to make the survey measurement of the azimuth and elevation angles and the radial distances to the mirrors relative to the OP-FTIR sensor. ARCADIS had the following tasks:

- Collect OP-FTIR data in order to identify major emissions hot spots by generating surface concentration maps in the horizontal plane
- Measure emission fluxes of detectable compounds downwind from major hot spots
- Collect any ancillary data
- Demonstrate the operation and function of the ORS technology

Additionally, U.S. EPA personnel operated a bistatic, non-scanning OP-FTIR (manufactured by Midac) to determine ambient background concentrations, and these measurements were used to correct the results of the ORS-RPM measurements for background contributions of the analytes. The following sections provide general descriptions of the experiments performed at the site.

1.2.1 Horizontal Radial Plume Mapping

The RPM approach provides spatial information to path-integrated measurements by optical remote sensing. This technique yields information on the two-dimensional distribution of the concentrations in the form of chemical-concentration contour maps (Hashmonay et al., 1999; Wu et al., 1999; Hashmonay et al., 2002). This form of output readily identifies chemical “hot spots,” the location of high emissions. This method can be of great benefit for performing site surveys prior to site remediation activities.

Horizontal radial scanning is usually performed with the ORS beams located as close to the ground as practical. This enhances the ability to detect minor constituents emitted from the ground, since the emitted plumes dilute significantly at higher levels above the ground. The survey area is divided into a Cartesian grid of n times m rectangular cells. A mirror is located in each of these cells and the OP-FTIR sensor scans to each of these mirrors, dwelling on each for a set measurement time (30 seconds in the present study). The system scans to the mirrors in the order of either increasing or decreasing azimuth angle. The path-integrated concentrations measured at each mirror are averaged over a several scanning cycles to produce time-averaged concentration maps. Meteorological measurements are made concurrent with the scanning measurements.

Figure 1-2 represents a typical horizontal RPM configuration in which $n = m = 3$. The lines represent the nine optical paths, each terminating at a mirror (Hashmonay et al., 2002). The solid square represents a point source. The enclosed areas represent the calculated plume, transported down-wind by the wind. The numbers associated with the isopleths are the determined values for the concentrations. Horizontal scanning was performed at the five survey areas depicted in Figure 1-1.

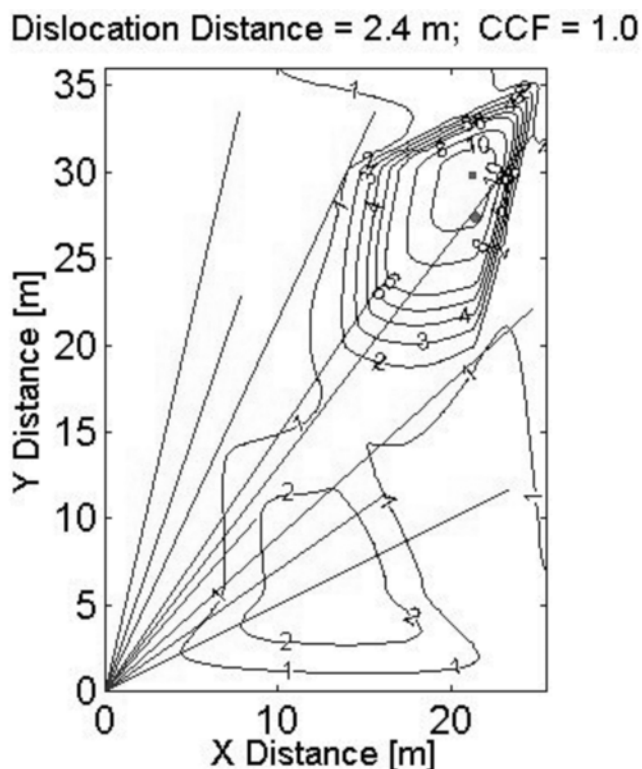


Figure 1-2. Overhead View of an Example Horizontal RPM Configuration.

1.2.2 Vertical Radial Plume Mapping

The vertical RPM method maps the concentrations in the vertical plane of the measurement. By scanning in a vertical plane downwind from an area source, one can obtain plume concentration profiles and calculate the plane-integrated concentrations. The flux is calculated by multiplying the plane-integrated concentration by the wind speed component perpendicular to the vertical plane. The flux leads directly to a determination of the emission rate (Hashmonay et al., 1998; Hashmonay and Yost, 1999, Hashmonay et al., 2001). Thus, vertical scanning leads to a direct measurement-based determination of the upwind source emission rate. At the Somersworth Superfund Site, a vertical scanning measurement was performed at the eastern boundary (See Figure 1-1).

Figure 1-3 shows a schematic of the experimental setup used for vertical scanning. Several mirrors are placed in various locations on a vertical plane in-line with the scanning OP FTIR. Two of the mirrors used in the configuration are mounted on a scissors jack (which is a piece of equipment used to create a vertical platform for mounting mirrors in the configuration). The location of the vertical plane is selected so that it intersects the mean wind direction as close to perpendicular as practical. Vertical scanning was performed on the down-wind side of the Somersworth Superfund site (the eastern border in Figure 1-1), in order to estimate a methane flux for the entire site.

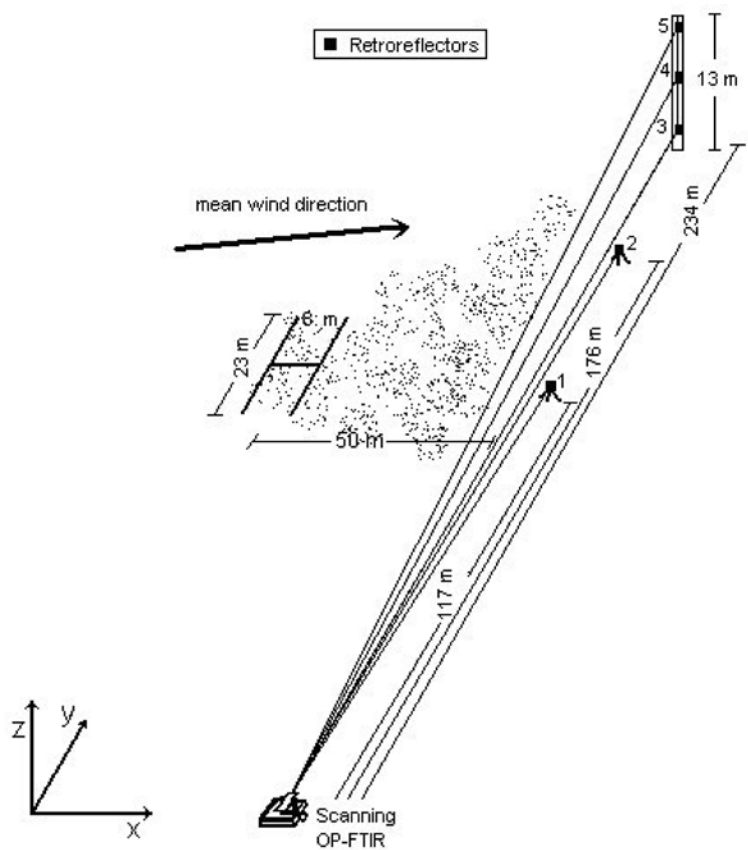


Figure 1-3. Example of a Vertical RPM Configuration

1.3 Data Quality Objectives and Criteria

Data quality objectives (DQOs) are qualitative and quantitative statements developed using EPA's DQO Process (described in *EPA QA/G-4, Guidance for the Data Quality Objectives Process*) that clarify study objectives, define the appropriate type of data, and specify tolerable levels of potential decision errors that will be used as the basis for establishing the quality and quantity of data needed to support decisions. DQOs define the performance criteria that limit the probabilities of making decision errors by considering the purpose of collecting the data, defining the appropriate type of data needed, and specifying tolerable probabilities of making decision errors. For this project, the qualitative data quality objective is to provide data to support the state in a risk assessment decision regarding this site.

Quantitative objectives are established for critical measurements using the data quality indicators of accuracy, precision, and completeness. The acceptance criteria for these data quality indicators are summarized in Table 1-1. Accuracy of measurement parameters is determined by comparing a measured value to a known standard. Values must be within the listed tolerance to be considered acceptable. Accuracy can also be measured by calculating the percent bias of a measured value to that of a true value.

Precision is evaluated by making replicate measurements of the same parameter and then assessing the variations of the results. Replicate measurements are expected to fall within the tolerances shown in Table 1-1. Completeness is expressed as a percentage of the number of valid measurements compared to the total number of measurements taken.

Table 1-1. DQI Goals for Critical Measurements

Measurement Parameter	Sampling Method(s)	Analysis Method	Accuracy	Precision	% Complete
Wind direction	N/A	Magnetic compass with vane	±5° tolerance	±5°	90%
Wind speed	N/A	Heavy duty wind cup set	±0.8 m/s	±0.8 m/s	90%
Optical path length	N/A	Theodolite	±1 m	±1 m	100%
Mid-IR absorbance	N/A	FTIR	±10%	±10% abs	90%

ORS-RPM was used at each test site to evaluate fugitive emissions of the target compounds, if detectable. Estimated minimum detection limits, by compound, are given in Table 1-2. It is important to note that the values listed in Table 1-2 should be considered first step approximations, as the minimum detection limit is highly variable, and depends on many factors including atmospheric conditions. Actual minimum detection levels are calculated in the quantification software for all measurements taken. Minimum detection levels for each absorbance spectrum are determined by calculating the root mean square (RMS) absorbance noise in the spectral region of the target absorption feature. The minimum detection level is the absorbance signal (of the target compound) that is five times the RMS noise level using a reference spectrum acquired for a known concentration of the target compound.

Table 1-2. Detection Limits for Target Compounds

Compound	Sampling/ Analytical Method	Estimated Detection Limits for 100 m One-Way Path, 1 min Average (ppmv)
Acetaldehyde	FTIR	0.010
Acetone	FTIR	0.024
Acrylonitrile	FTIR	0.010
Benzene	FTIR	0.040
Bromodichloromethane	FTIR	N/A
1,3-Butadiene	FTIR	0.012
Butane	FTIR	0.006
Carbon disulfide	FTIR	0.028
Carbon tetrachloride	FTIR	0.008
Carbonyl sulfide	FTIR	0.006
Chlorobenzene	FTIR	0.040
Chloroform	FTIR	0.012
Chloromethane	FTIR	0.012
1,4-Dichlorobenzene	FTIR	0.012
Dichlorodifluoromethane	FTIR	0.004
t-1,2-Dichloroethene	FTIR	N/A
Dichlorofluoromethane	FTIR	N/A
Dimethyl sulfide	FTIR	0.018
Ethane	FTIR	0.010
Ethanol	FTIR	0.006

(Continued)

Table 1-2. Detection Limits for Target Compounds (continued)

Compound	Sampling/ Analytical Method	Estimated Detection Limits for 100 m One-Way Path, 1 min Average (ppmv)
Ethyl benzene	FTIR	0.060
Ethyl chloride	FTIR	0.004
Ethyl mercaptan	FTIR	N/A
Ethylene dibromide	FTIR	0.006
Ethylene dichloride	FTIR	0.030
Fluorotrichloromethane	FTIR	0.004
Formaldehyde	FTIR	0.006
Hexane	FTIR	0.006
Hydrogen sulfide	FTIR	6.0
Methane	FTIR	0.024
Methyl chloroform	FTIR	0.006
Methyl ethyl ketone	FTIR	0.030
Methyl isobutyl ketone	FTIR	0.040
Methyl mercaptan	FTIR	0.060
Methylene chloride	FTIR	0.014
Pentane	FTIR	0.008
Propane	FTIR	0.008
2-Propanol	FTIR	0.006
Propylene dichloride	FTIR	0.014
Tetrachloroethene	FTIR	0.004
Toluene	FTIR	0.040
Trichlorethylene	FTIR	0.004
Vinyl chloride	FTIR	0.010
Vinylidene chloride	FTIR	0.014
Xylenes	FTIR	0.030

1.4 Schedule of Work Performed for Project

One field measurement campaign was completed for this project. The field tests were performed at the site during the end of September and beginning of October 2002 and were completed in six days (three days at the site and three days traveling to and from the site). Table 1-3 provides the schedule of work that was performed for each day of the project.

Table 1-3. Schedule of Work Performed for Somersworth, NH Field Study

Date	Day of Week	Detail of Work Performed
29 September 2002	Sunday	Transport equipment to site
30 September 2002	Monday	AM: Arrive at site PM: Horizontal scanning of Area A (1.5 hours)
1 October 2002	Tuesday	Horizontal scanning of Area B (2 hours), Area D (2 hours), and Area E (1 hour)
2 October 2002	Wednesday	Horizontal scanning of Area B (2 hours) and vertical scanning
3 October 2002	Thursday	Transport equipment from site
4 October 2002	Friday	Continue travel with equipment

2.0

The Measurements

The following subsections describe testing procedures done at each of the five survey areas, which are designated as Area A through Area E. Each site was scanned horizontally to produce concentration maps and to locate any hot spots. In addition, a vertical scanning survey was done on the eastern side of the site. In each of these sections, a figure is included that details the respective survey area. The location of the vertical scanning configuration is depicted in Figure 1-1. The square shows the location of the scissors jack, the dot shows the location of the scanner/OP-FTIR instrument, and the dashed line indicates the position of the vertical plane.

2.1 Area A

Area A is located in the northwestern section of the landfill site. A line of large trees bounds the survey area on the northern side (see Figure 1-1). Figure 2-1 shows a schematic of the horizontal scanning configuration in Area A, which was divided into nine cells located as in Figure 2-1. The scanning OP-FTIR sensor was setup in the southeast corner of Cell 1 in Area A. In the RPM calculations, the boundaries of Cells 8 and 9 were altered to accommodate the tree-lined fence. Table 2-1 lists the radial coordinates (relative to the OP-FTIR sensor) for each of the nine mirrors.

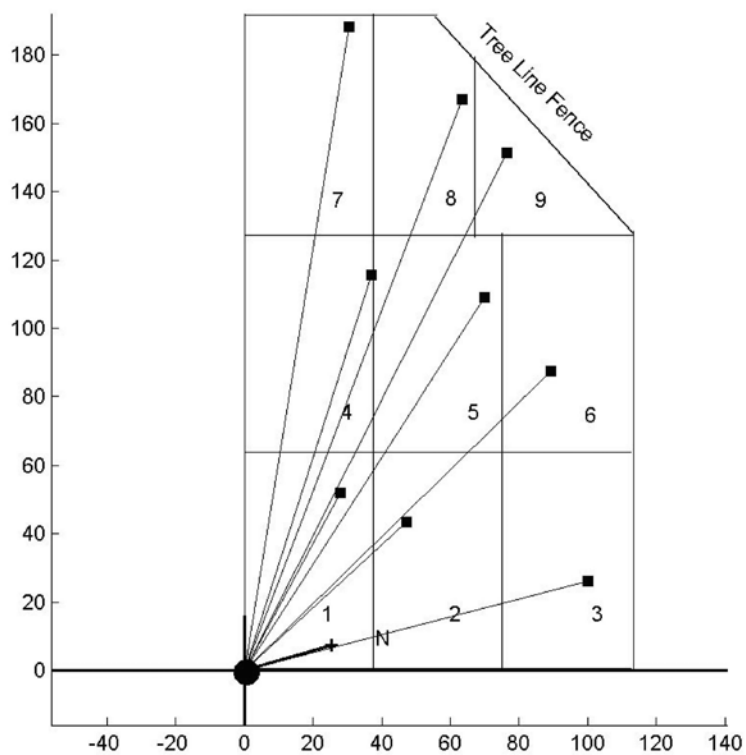


Figure 2-1. Schematic of OP-FTIR RPM Measurement Configuration in Area A (distances in meters).

Table 2-1. Coordinates of Mirrors Used for Horizontal Scanning in Area A.

Mirror Number	Radial Distance ^a (m)	Azimuth Angle from North ^a (deg)
1	58.9	315
2	64.1	334
3	103	2
4	121	304
5	130	320
6	125	332
7	191	296
8	179	307
9	170	313

^a The radial distance and azimuth are relative to the position of the scanning OP-FTIR.

2.2 Area B

Area B is located in the southeastern section of the site, includes a baseball field and basketball courts (see Figure 1-1), and is divided into 11 cells. Figure 2-2 is a schematic of the horizontal scanning configuration in Area B and shows the scanning OP-FTIR sensor was setup in the northwest corner of the area. A second monostatic (Unisearch) OP-FTIR system was setup four meters from the scanning OP-FTIR and made simultaneous measurements over two paths to the mirror positions shown in Figure 2-2 for Cells 10 and 11. These measurements were combined with those made to the nine cells by the scanning system, resulting in an eleven-cell RPM computation. Table 2-2 lists the radial coordinates (relative to the OP-FTIR sensor) for each of the nine mirrors.

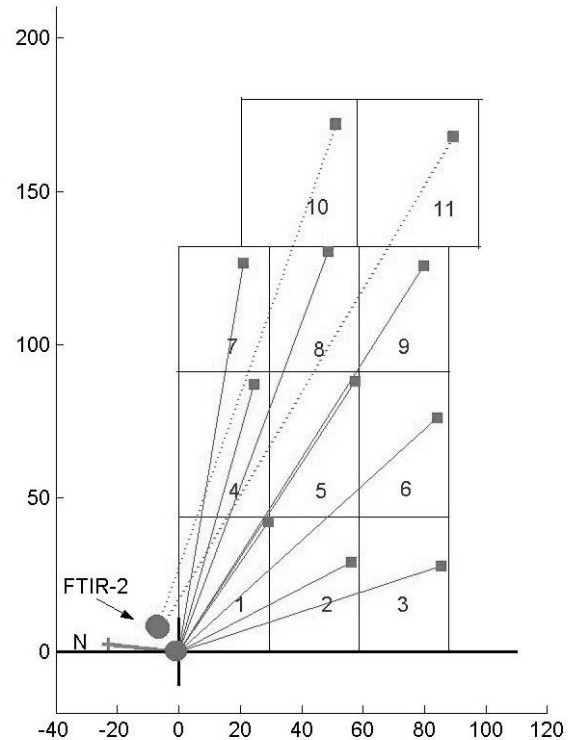


Figure 2-2. Schematic of OP-FTIR RPM Measurement Configuration in Area B (distances in meters).

Table 2-2. Coordinates of Mirrors Used for Horizontal Scanning in Area B.

Mirror Number	Radial Distance ^a (m)	Azimuth Angle from North ^a (deg)
1	51.4	119
2	63.4	147
3	89.8	156
4	90.4	100
5	105	117
6	114	132
7	128	93
8	139	104
9	149	116
10	219	97
11	219	119

^a The radial distance and azimuth are relative to the position of the scanning OP-FTIR.

2.3 Area C

Area C is located in the northern section of the site and includes a baseball field (see Figure 1-1). Figure 2-3 is a schematic of the horizontal scanning configuration in Area C and shows the scanning OP-FTIR sensor set up in the southeastern corner of the area. A fence cut across the northwest corner of the area, resulting in locating some of the mirrors in less than optimum positions for the RPM algorithm. The radial coordinates are given for all nine mirrors in Table 2-3.

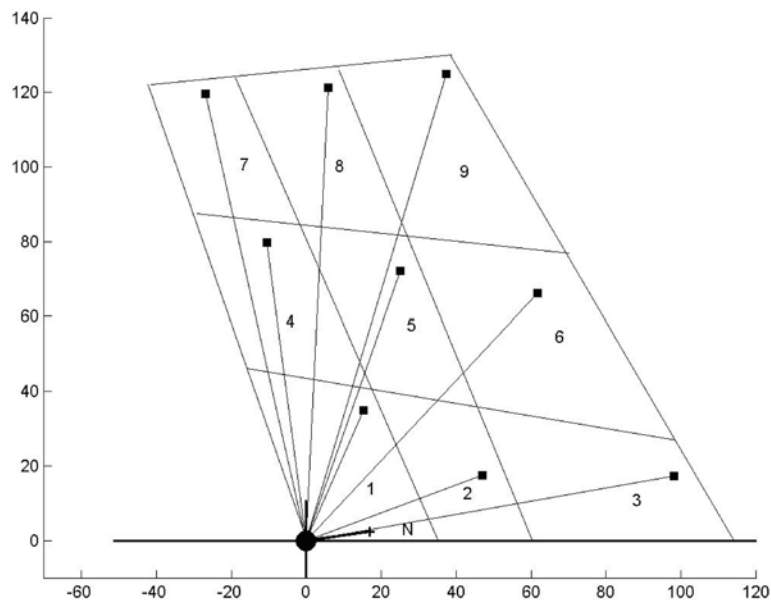


Figure 2-3. Schematic of OP-FTIR RPM Measurement Configuration in Area C (distances in meters).

Table 2-3. Coordinates of Mirrors Used for Horizontal Scanning in Area C.

Mirror Number	Radial Distance ^a (m)	Azimuth Angle from North ^a (deg)
1	38.1	301
2	50.1	347
3	99.6	358
4	80.5	270
5	76.4	297
6	90.5	321
7	123	265
8	122	281
9	131	295

^a The radial distance and azimuth are relative to the position of the scanning OP-FTIR.

2.4 Area D

Area D is inside the chain-link fence of four tennis courts in the northeastern corner of the landfill site (see Figure 1-1). Figure 2-4 is a schematic of the horizontal scanning configuration in Area D and shows the setup in this area was different from the other areas in that the scanning OP-FTIR sensor was located on the center of one side, instead of a corner, of the rectangular area. The scanning sensor was located on the western side of Area D. Since Area D was confined by a chain-link fence, it was much smaller than the other survey areas in the study. The coordinates of the nine mirrors are listed in Table 2-4.

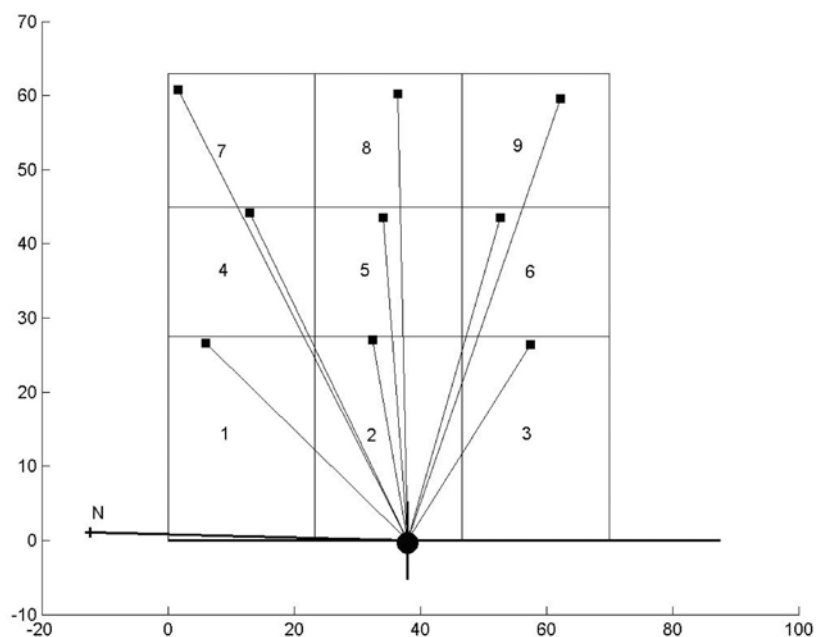


Figure 2-4. Schematic of OP-FTIR RPM Measurement Configuration in Area D (distances in meters).

2.5 Area E

Area E is located in the southwestern section of the site (see Figure 1-1). Figure 2-5 shows a schematic of the horizontal scanning configuration in Area E. The scanning OP-FTIR sensor was setup in the northeastern corner of the designated area, and only four mirrors were used. The coordinates of the four mirrors are listed in Table 2-5.

Table 2-4. Coordinates of Mirrors Used for Horizontal Scanning in Area D.

Mirror Number	Radial Distance ^a (m)	Azimuth Angle from North ^a (deg)
1	41.6	35
2	27.6	73
3	32.8	121
4	50.8	55
5	43.7	80
6	46.1	104
7	70.9	54
8	60.2	83
9	64.3	107

^a The radial distance and azimuth are relative to the position of the scanning OP-FTIR.

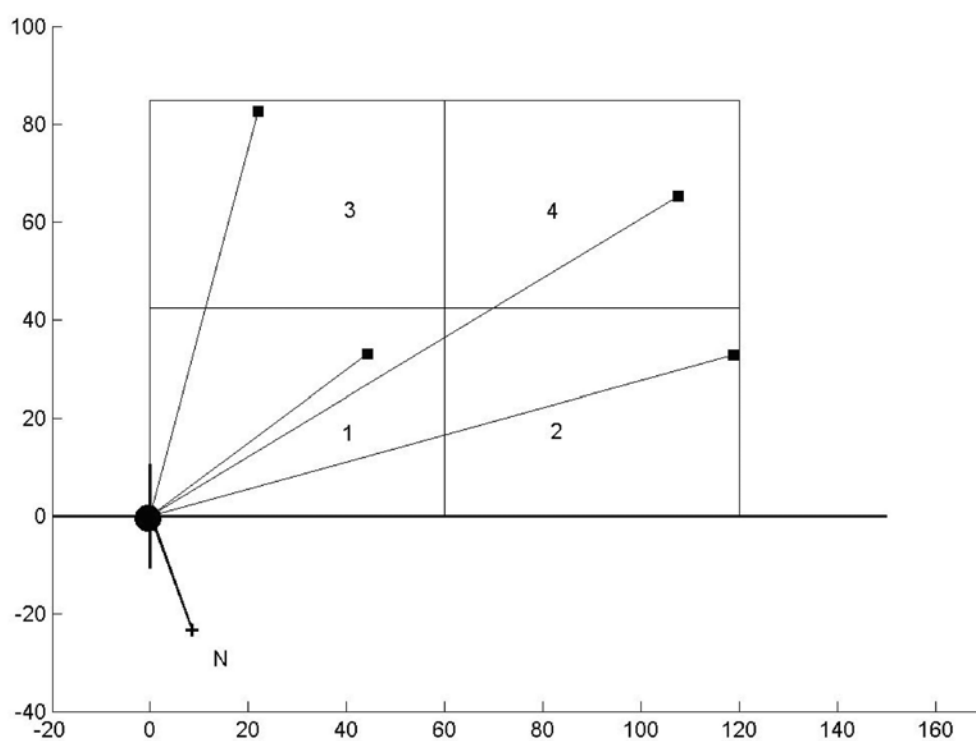


Figure 2-5. Schematic of OP-FTIR RPM Measurement Configuration in Area E (distances in meters).

Table 2-5. Coordinates of Mirrors Used for Horizontal Scanning in Area E.

Mirror Number	Radial Distance^a (m)	Azimuth Angle from North^a (deg)
1	55.3	253
2	123	275
3	85.5	215
4	126	259

^a The radial distance and azimuth are relative to the position of the scanning OP-FTIR.

2.6 Vertical Scanning

The vertical scan configuration was set up along the eastern boundary of the landfill site. This location was chosen because it was optimum under the given wind condition for determining a methane flux that would be representative of the entire site. Figure 1-1 shows the location of the vertical scanning configuration (the line shows the location of the vertical plane, the dot shows the location of the scanner/OP-FTIR, and the square shows the location of the scissors jack). The angular coordinates of the five mirrors are listed in Table 2-6.

Table 2-6. Coordinates of Mirrors Used for Vertical Scanning.

Mirror Number	Radial Distance^a (m)	Elevation Angle^b (deg)	Azimuth Angle from North^a (deg)
1	47.1	0	6
2	109	0	1
3	110	2	2
4	111	6	1
5	186	0	2

^a The radial distance and azimuth are relative to the position of the scanning OP-FTIR.

^b Elevation angle shown is the angle from the horizontal axis to the mirror.

2.7 Meteorological Data

Meteorological data, including wind direction, wind speed, temperature, relative humidity, and barometric pressure, were continuously collected during the sampling campaign with a Climatronics weather station, model 101990-G1. The weather station collects real-time data from its sensors and records time-stamped data to a data logger.

Wind direction and speed-sensing heads were used to measure the wind speed and direction at height of 2 and 10 meters. The sensing heads for wind direction incorporate an automatic sensing function that adjusts to true north, eliminating the errors associated with using a compass heading. The sensing heads incorporate standard cup-type wind speed sensors.

2.8 Data Analysis

The OP-FTIR data were collected as interferograms and archived to CD-ROMs. The archived interferograms were delivered to U.S. EPA personnel, who performed the conversions to absorbance spectra, which they analyzed to determine concentrations using Non-Lin (Spectrosoft) software. This analysis was done after completion of the field campaign. The concentration determinations were combined with the appropriate mirror locations, wind speed, and wind direction, and algorithms developed in MatLab (Math-works) were then used to process the data into horizontal plane concentration maps or vertical plane plume profiles. The fluxes were then determined as the product of the determined area-integrated concentrations times the component of the wind speed normal to the vertical measurement plane.

Copies of the interferogram data were also analyzed by ARCADIS. These spectra files were searched for volatile organic compounds (VOCs) and ammonia concentrations, and EPA's methane-concentration determinations were verified.

3.0

Analytical Results and Discussion

The RPM algorithm is the tool that extracts the spatial information from the open-path measurements to produce plume concentration maps and emission rates. The concordance correlation factor (CCF) is used to represent the level of fit for the reconstruction in the path-integrated domain (predicted vs. observed PIC) (Hashmonay et. al, 1999). The CCF is similar to the Pearson correlation coefficient but is adjusted to account for shifts in location and scale. Like the Pearson correlation, CCF values are bounded between -1 and 1, yet the CCF can never exceed the absolute value of the Pearson correlation factor. For example, the CCF will be equal to the Pearson correlation when the linear regression line intercepts the ordinate at 0, its slope equals 1, and its absolute value will be lower than the Pearson correlation when these conditions are not met. For the purposes of this report, the closer the CCF value is to 1, the better the fit for the reconstruction in the path-integrated domain.

In reporting the average calculated fluxes, a moving average is used in Table 3-1 to show temporal variability in the flux values. A moving average involves averaging flux values calculated from several different consecutive cycles (a cycle is defined as data collected when scanning one time through all the mirrors in the configuration). For example, a data set taken from five cycles may be reported using a moving average of four, where values from cycle one to four and two to five are averaged together to show any variability in the flux values.

3.1 The Horizontal RPM Results

Figures 3-1 through 3-5 present the average reconstructed methane concentrations for Areas A through E, respectively. The contours give methane concentrations in ppmv, and the Xs show the positions of the mirrors. The corresponding schematic diagrams of each area provide directional indicators. Additionally, the calculated CCF for each reconstruction is provided. Table 3-2 shows a list of the area-averaged concentrations of methane in all of the 42 cells measured in the 5 areas. The table also includes five auxiliary measurements taken with the Unisearch OP-FTIR within Cell 10 of Area B. These additional measurements were taken to provide more detailed spatial information on the hot spot detected in this area. The listed methane values are area

averages for each of the cells as computed by the RPM algorithms. The global methane background value of 1.75 ppm was subtracted from each of the area-averaged values. The highest methane area-averaged concentrations were measured in Cell 8 (3.06 ppm) in Area C and Cells 1 and 2 in Area A (2.64 ppm and 2.69 ppm, respectively, see Figures 2-1 and 2-3). The methane levels in these three cells were more than 2.5 ppm higher than the global background level of 1.75 ppm. The area-averaged determinations for methane in the other 39 cells ranged from the ambient background level to 2.27 ppm above background. The mean value of all 42 determinates was 1.03 ppm.

Table 3-1. Moving Average of Calculated Methane Flux, CCF, Wind Speed, and Wind Direction for the Vertical Scanning Survey.

Cycles	CCF	Flux (g/s)	Wind Speed (m/s)	Wind Direction^a (deg)
1 to 4	0.999	4.4	2.23	7
2 to 5	0.998	5.2	2.32	3
3 to 6	0.998	5.5	2.27	0
4 to 7	0.993	5.1	2.42	0
5 to 8	0.992	6.0	2.78	1
6 to 9	0.985	6.5	2.73	3
7 to 10	0.985	7.1	2.78	1
8 to 11	0.994	8.7	2.72	356
9 to 12	0.994	7.7	2.41	345
10 to 13	0.997	6.4	2.29	340
11 to 14	0.999	5.1	2.11	333
Average	0.994	6.1	—	—
St. Dev. of Mean	0.0051	1.28	—	—

^a Wind direction shown is the angle from a vector normal to the plane of the configuration.

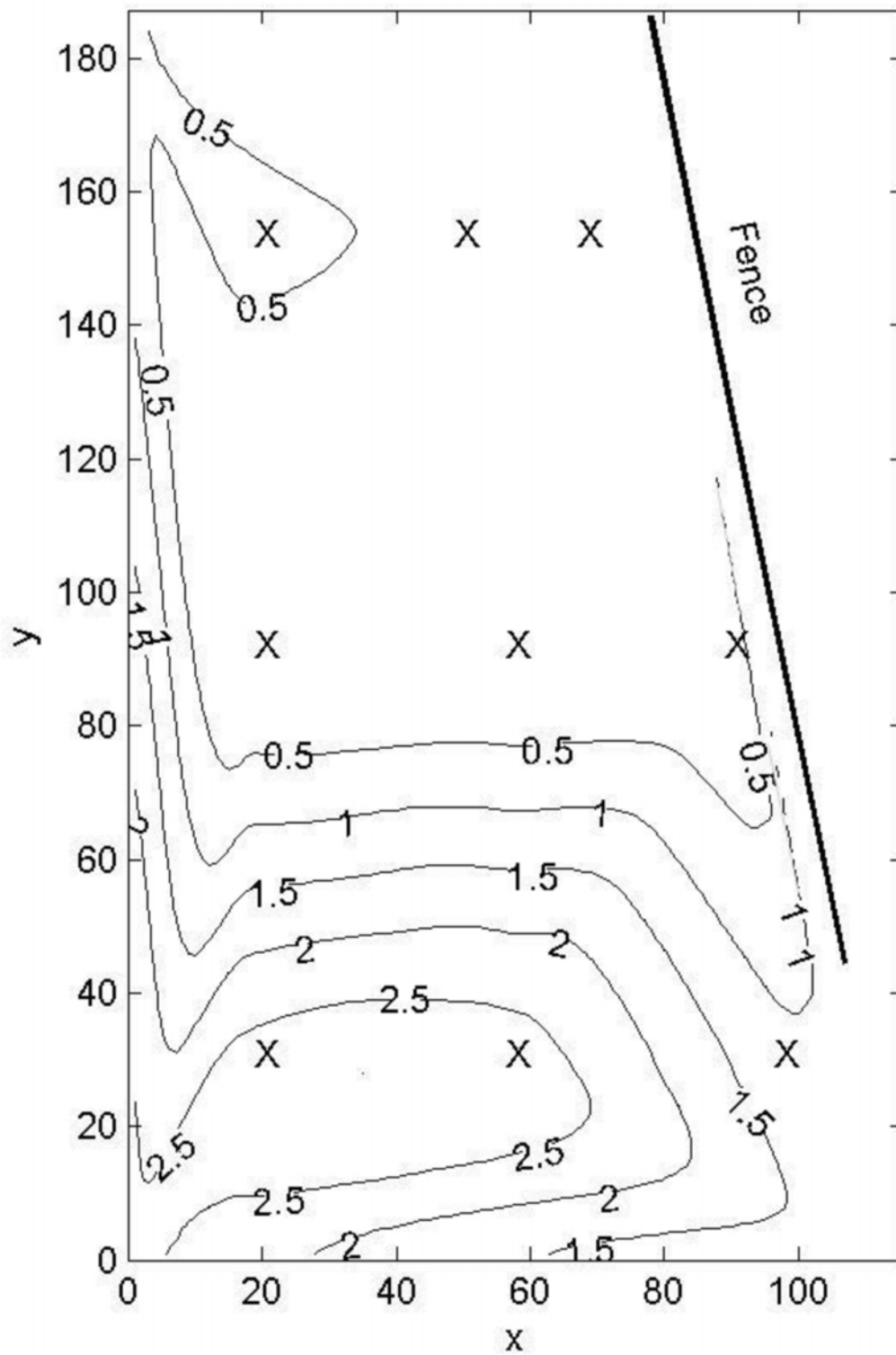


Figure 3-1. Reconstructed Methane Concentrations (in ppmv) for Area A (distances in meters).

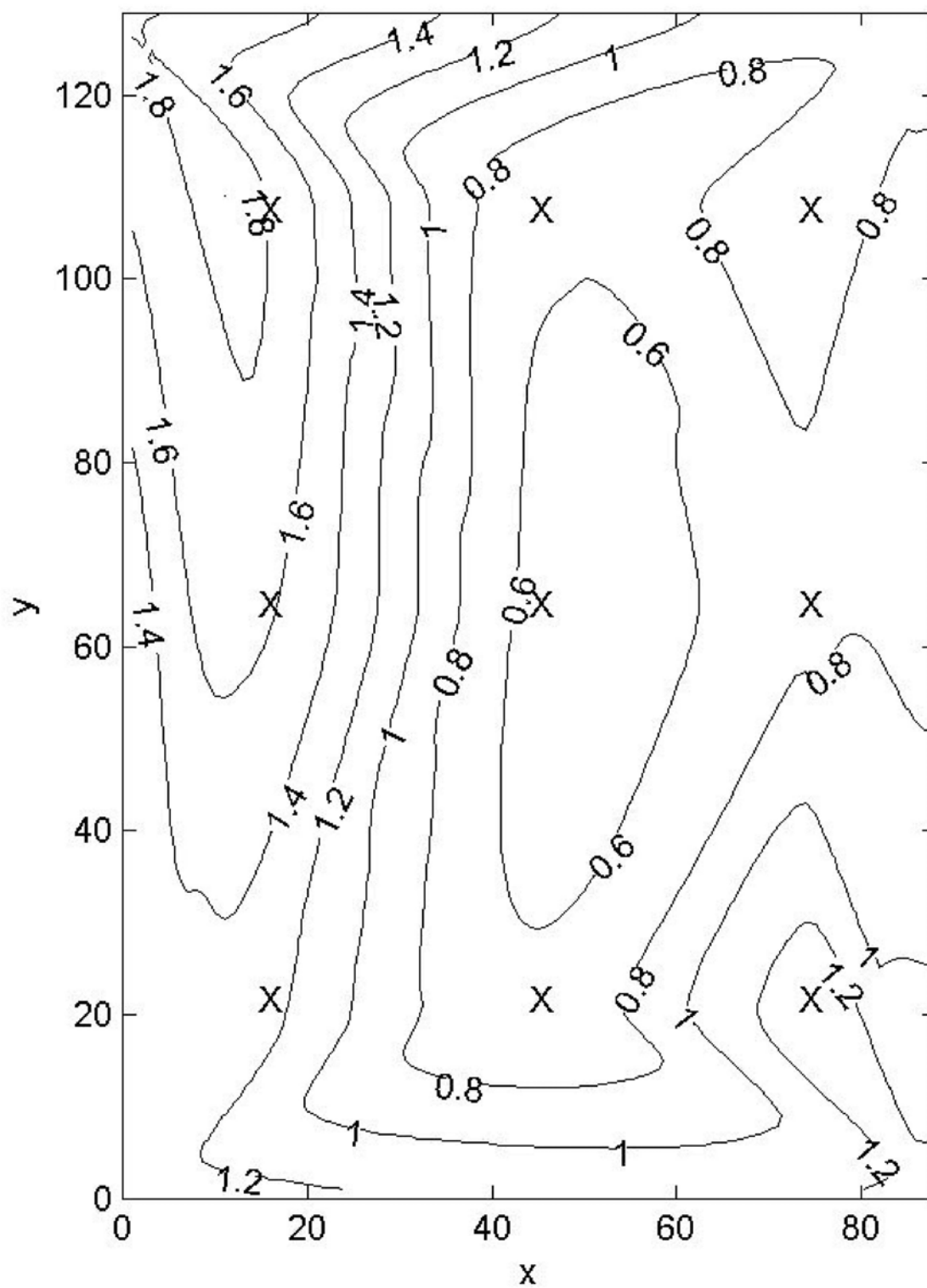


Figure 3-2. Reconstructed Methane Concentrations (in ppmv) for Area B (distances in meters).

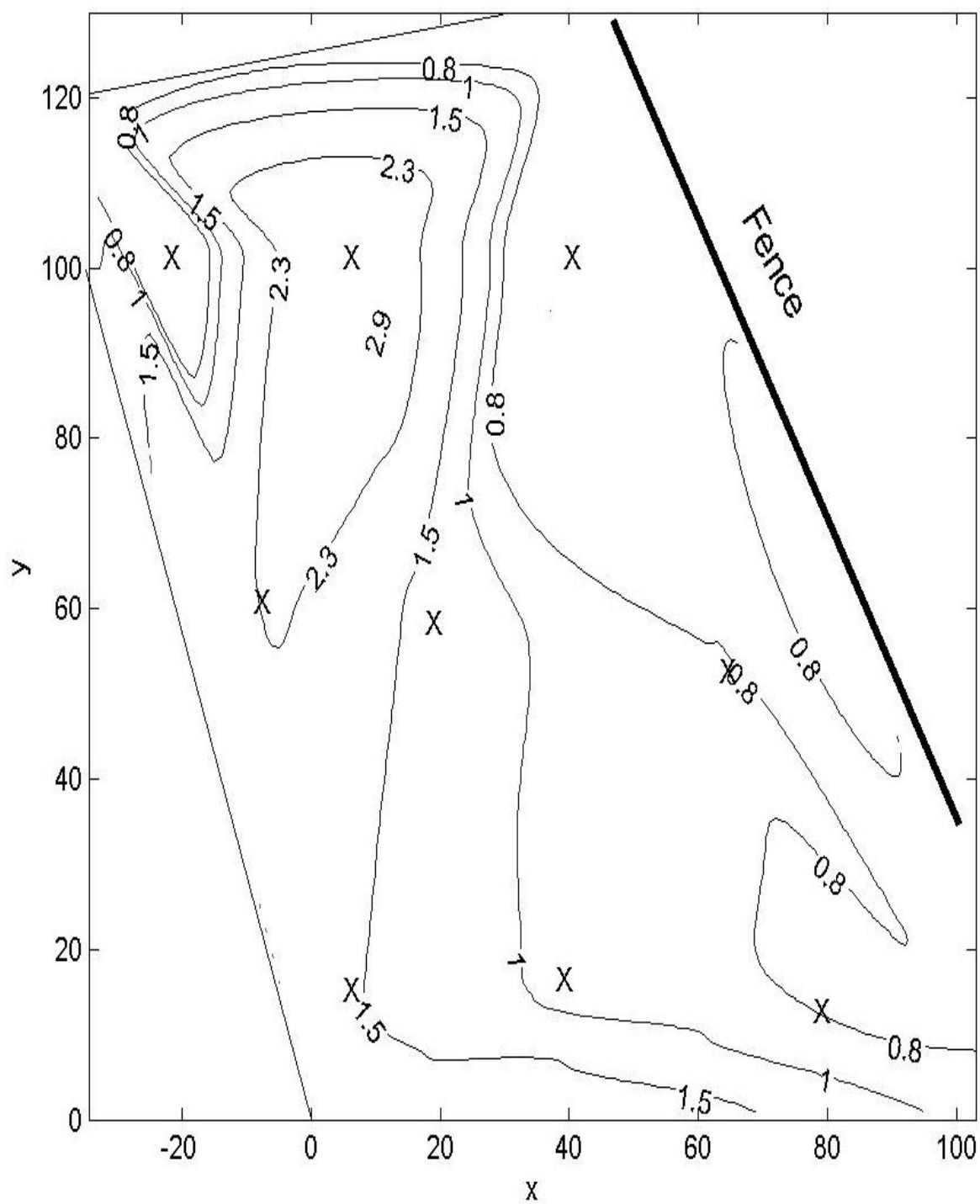


Figure 3-3. Reconstructed Methane Concentrations (in ppmv) for Area C (distances in meters).

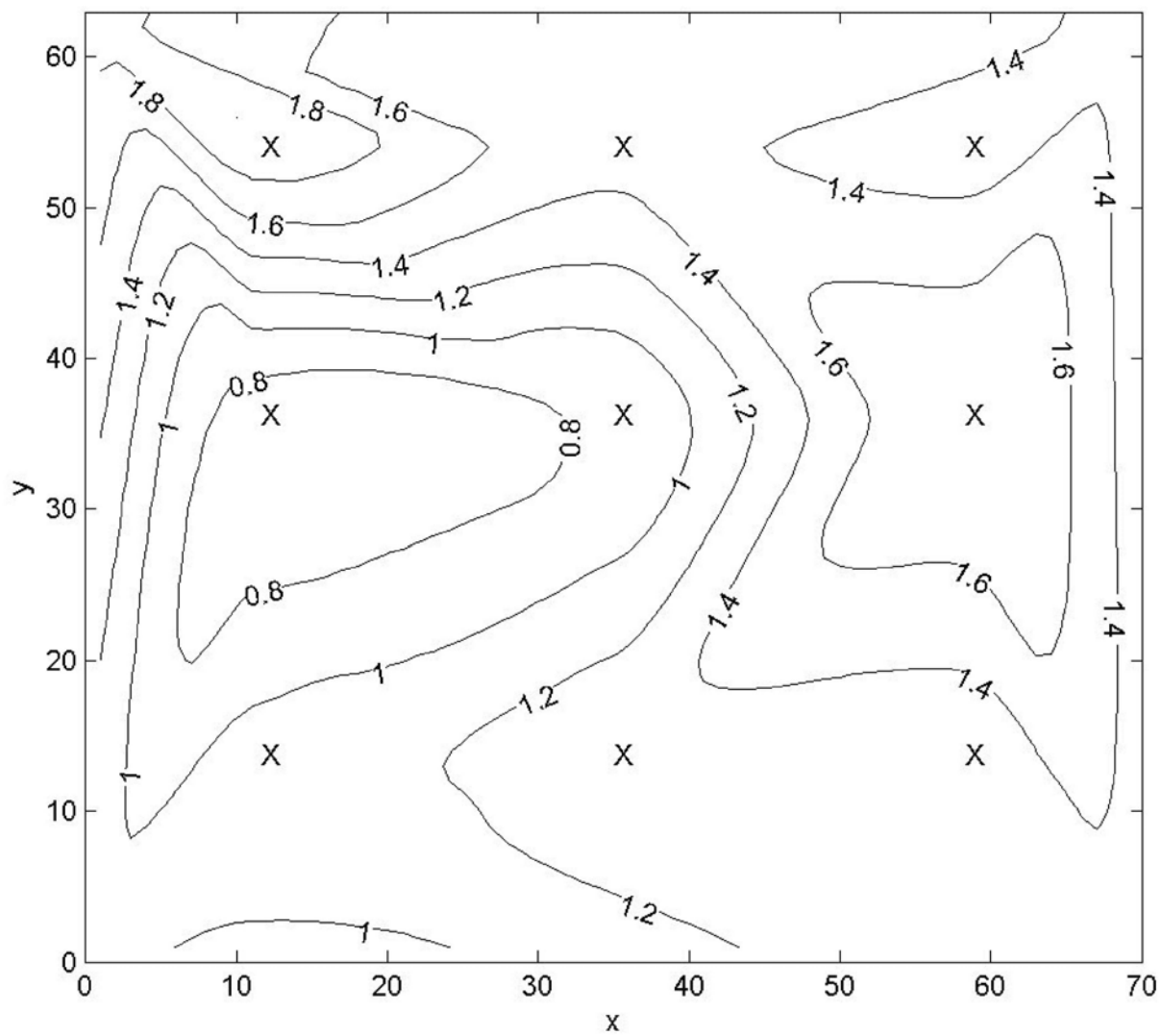


Figure 3-4. Reconstructed Methane Concentrations (in ppmv) for Area D (distances in meters).

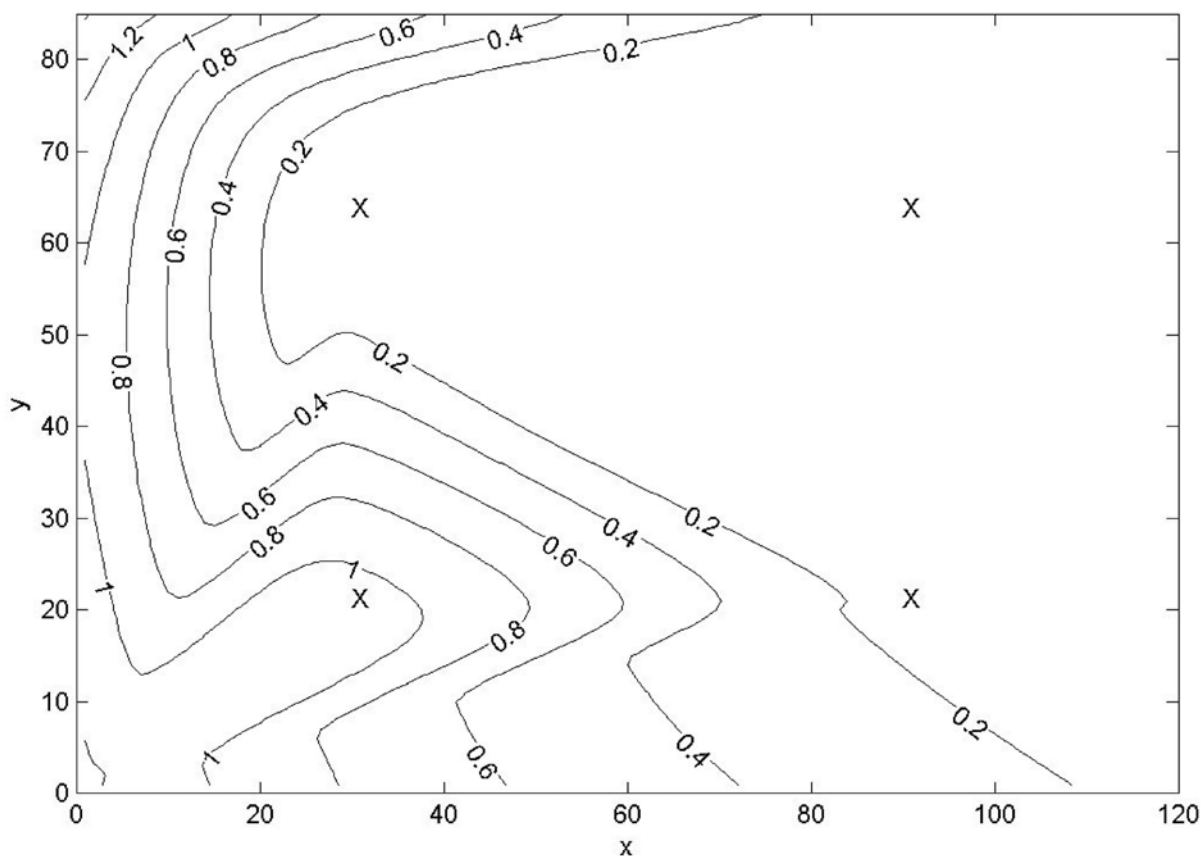


Figure 3-5. Reconstructed Methane Concentrations (in ppmv) for Area E (distances in meters).

Table 3-2. Mean Methane Concentration (ppm) Determinations for Each Area.

Cell Number	Area A	Area B	Area B Auxiliary Measurements	Area C	Area D	Area E
1	2.6	1.3	1.5	1.6	1.1	1.1
2	2.7	0.65	0.00	0.95	1.3	0.15
3	1.2	1.3	1.7	0.77	1.3	1.4
4	0.00	1.6	6.4	2.3	0.72	0.00
5	0.00	0.56	5.8	1.4	0.85	
6	0.00	0.75		0.79	1.8	
7	0.62	1.8		0.00	1.9	
8	0.33	0.68		3.1	1.5	
9	0.00	0.92		0.00	1.3	
10		1.1				
11		0.31				

Figure 3-6 shows RPM-determined methane concentration contours overlaid on a site map of the Somersworth landfill. The dots indicate the OP-FTIR locations used to collect the data. The determination of this concentration map is based solely on the mean path-integrated measurements in the five areas comprising a total of 42 cells and 5 auxiliary path-integrated measurements made by the Unisearch OP-FTIR in Area B. The methane concentration map shows three hot spots, one in Area A (2.5 ppm above ambient), the second in the north west corner of Area C (3.0 ppm above ambient), and the third hot spot, the most intense at 6.5 ppm above ambient, occurred in the small valley north of the baseball field in Area B. Since this hot spot was identified in Area B, the Unisearch OP-FTIR was setup in the valley and made path-integrated measurements to five mirror positions in, and on, the north and south slopes of the valley. Including the five path-integrated measurements from the Unisearch instrument in the RPM calculation provided the detail showing the sharp concentration gradients shown in Figure 3-6. The Unisearch measurements located strong methane emissions from an uncapped vent (probably from a hole dug for a utility pole that was never installed) located on the south slope of the valley adjacent to the Area B ball field.



Figure 3-6. The OP-FTIR RPM Methane Concentration Contours Overlaid on the Map of the Somersworth Superfund Landfill.

3.2 The Vertical RPM Results

Table 3-1 presents methane emission flux determinations from the vertical scanning survey. See Figure 1-1 for the location of the vertical scanning survey at the site. The first column of this table refers to a running average calculation from the several cycles. The second column shows the calculated CCF. The third, fourth, and fifth columns show the calculated methane flux, the average wind speed, and the wind direction, respectively, during the time the measurements were taken.

Figure 1-3 shows the schematic of the vertical scanning configuration. The measurement was set up on the eastern boundary that was on the downwind side of the landfill and located so that the centerline of the methane plume emitted from the hot spots in the valley and from Areas C and A would intersect the beam paths. The centerline of the plume was closer to the mirror tower than to the OP-FTIR sensor, and some of the plume extended beyond the tower. This portion of the plume was captured by the beam to mirror number 5, which was situated 186 meters from the sensor.

The emission flux was determined for the vertical-plane area shown in Figure 3-7 (186 meters horizontal and 23 meters vertical) by multiplying the area-integrated concentration by the component of the wind speed normal to the vertical plane. This resulted in a flux value of 5.8 g/sec. This vertical plane captured most of the methane plume emitted from the landfill; thus, the flux through this plane is approximately equal to the emission rate for the entire landfill.

The vertical scanning configuration shown in Figure 3-7 was situated just downwind of the location of high methane emissions in the valley, which is referred to as the hot spot. However, the vertical plane with the 186-meter horizontal distance extended sixty meters beyond the hot-spot plume. The vertical scan measurements can also be used to determine the emission flux from the hot spot by narrowing the RPM computation to the portion of the vertical plane through which the hot spot plume passes, as shown in Figure 3-8. The RPM determined flux for this modified plane, which extends to 140 meters from the OP-FTIR sensor, was 4.6 g/sec. This flux also includes contributions from the areas of the landfill that are upwind of the hot spot. To determine the net flux from the hot spot, a vertical plane configuration was set up immediately upwind, just west of the hot spot and collected data simultaneously. This configuration, which used two separate non-scanning OP-FTIR sensors, is shown in Figure 3-9. The flux through this plane was determined as 1.3 g/sec. The net flux through the 140-meter by 25-meter plane is the difference between the flux through the downwind plane and that of the upwind plane, 3.3 g/sec. Since the downwind plane contained the hot-spot plume, the mean emission rate from the hot

spot is estimated to be 3.3 g/sec, which represents 57 percent of the emission (5.8 g/sec) from the entire landfill.

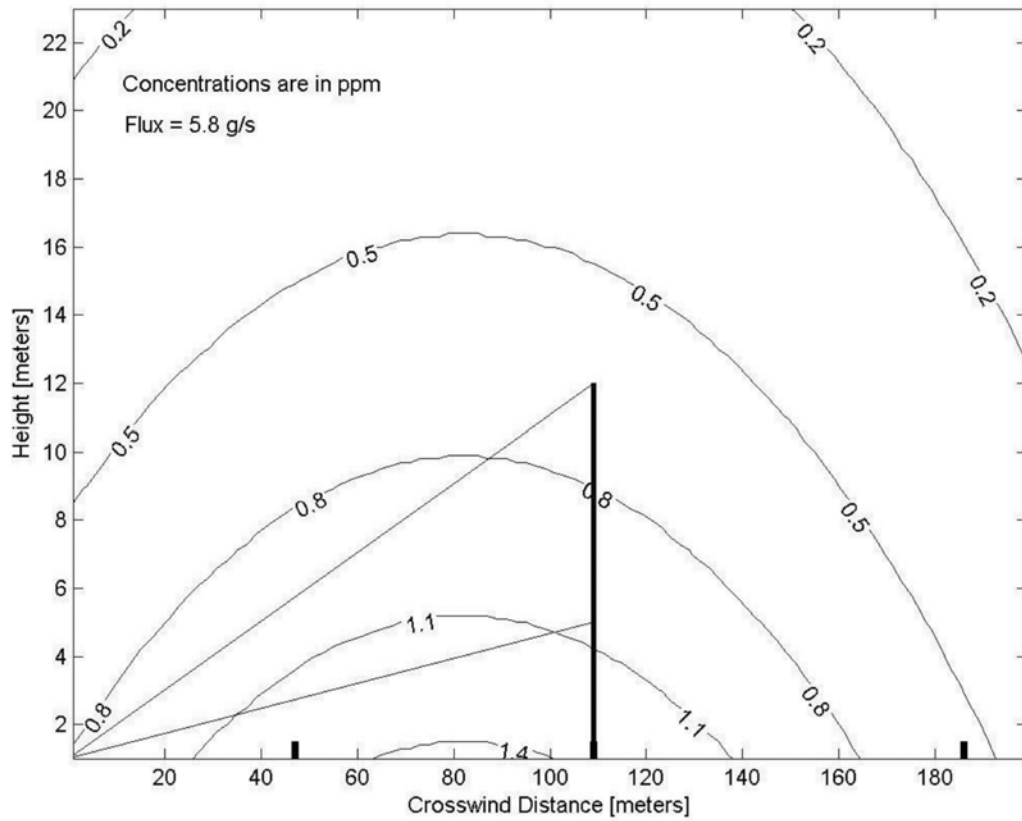


Figure 3-7. Vertical Scan RPM Measurement of the Vertical Methane Plume Profile (numbers on the isopleths are methane concentrations above the global background).

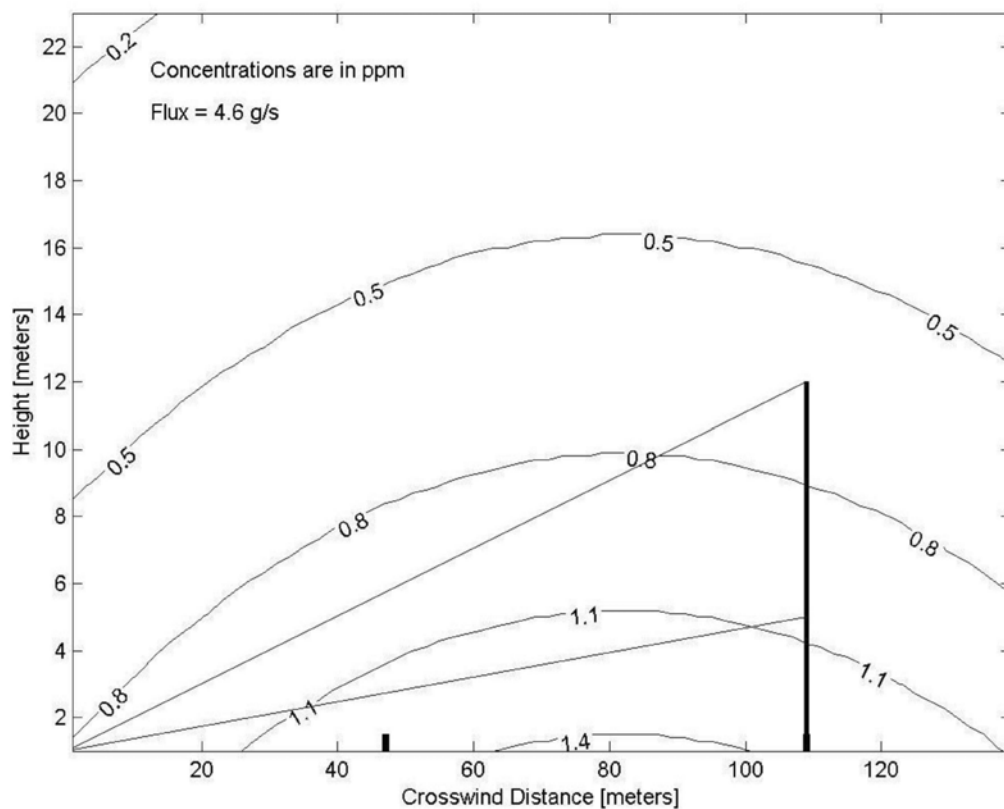


Figure 3-8. Vertical Scan RPM Measurement of the Plume Profile from the Hot Spot in the Valley (numbers on the isopleths are methane concentrations above the global background).

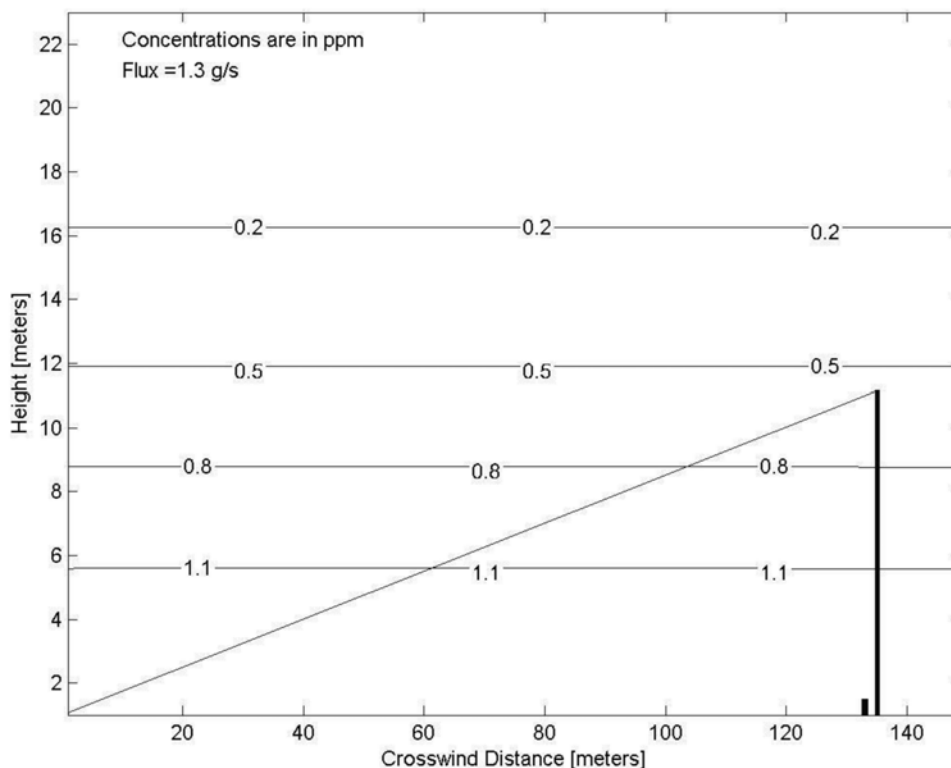


Figure 3-9. Two Beam RPM Measurement of the Vertical Methane Plume Profile on the Western (Upwind) Side of the Landfill (numbers on the isopleths are the methane concentrations above the global background).

3.3 The Search for HAPs and Other Chemicals

All regions of the spectra collected by both MIDAC and Unisearch Open-Path FTIRs were carefully searched for absorption features due to any chemicals that are normally not in the atmosphere. This search included all measurements on the 42 beams and from the vertical measurements as well as the Unisearch measurements near the methane hot spot in the valley. No absorption features were found. This result is not surprising, when one notes that the maximum concentration of methane measured at the landfill was 6.5 ppm. The minor constituents (neglecting the aliphatic hydrocarbons) occur at landfills at levels that are typically much less than 10^{-4} times the methane levels. Thus we would expect the minor constituents of the landfill gases to be lower than 650 pptv in the ground-level atmosphere, which are levels considerably lower than the detection limits of the OP-FTIR systems.

4.0

Quality Assurance/Quality Control

In preparation for this project, a Category III Quality Assurance Project Plan (QAPP) was prepared and approved prior to the field campaign. In addition, standard operating procedures were in place during the survey.

4.1 Assessment of DQI Goals

The data quality objectives established for critical measurements using the data quality indicators (DQIs) of accuracy, precision, and completeness are listed in Table 1-1 of this document. However, the goal is to develop improved DQIs for the applied techniques used in this type of research project.

Although calibration of the Climatronics heads did not occur prior to the field study, both Climatronics heads were calibrated in March 2003 by the U.S. EPA/APPCD Metrology Lab (the previous calibration of both heads was in November 1999). All functions were checked during the March 2003 calibration, and the only adjustment made was an approximately 4° change to wind direction for one of the Climatronics heads. As shown in Table 1-1, accuracy within 5% is an acceptable range, and this variance will have very little bearing on the final flux estimate.

It should also be noted that the wind direction measurement is not as critical to the flux estimates as the wind speed measurement. Additionally, checks for agreement of the wind speed and wind direction measured from the two heads (2m and 10m) were done. While it is true that some variability in the parameters measured at both levels should be expected, this is a good first-step check for assessing the performance of the instruments.

It has been determined that the accuracy of the measured optical path-lengths (which are collected using the theodolite), as stated in the QAPP and by the manufacturer's specifications, are not crucial to our method. However, calibration of the theodolite was done in the field during May 2003. The optical path-length was checked by measuring a standard distance of 50 feet (15.24 meters). The same distance was measured twice using the theodolite and yielded

distances of 15.43 and 15.39 meters. These results fall well within the acceptable accuracy range stated in Table 1-1. The horizontal angle was checked by setting up two targets approximately 180° apart, measuring the two horizontal angles between the targets, and calculating the sum, which should be 360°. These angles were measured twice using the theodolite. The first test yielded a sum of 359°21'18", and the second test yielded a sum of 359°59'55". Both of these values fall well within the acceptable accuracy range stated in Table 1-1.

As a QC check of the accuracy of the OP_FTIR, we have verified the measurement of the known atmospheric background nitrous oxide concentration of around 320 ppbv from data taken with the monostatic OP-FTIR. It should be noted that 320 ppbv is an average value, as the atmospheric background value exhibits a slight seasonal variation. The data were taken from a sample of the actual data collected during the current field campaign. The average nitrous oxide concentration found was 337 ± 9.121 ppbv. This value falls within the accuracy goals stated in Table 1-1.

Additionally, DQI procedures for proper operation, as described in EPA Compendium method TO-16, and the OP-FTIR EPA Guidance Document were followed for this study. The development of DQI standards for this method is a future goal, and improved DQI standards will be included in future QAPP documents written using this method.

4.2 Ethylene Tracer Release

To verify the accuracy of the method used to calculate emission flux, a tracer gas was released during the vertical scanning survey. Ethylene was released through a soaker hose configuration located directly west of the vertical scanning survey. The wind direction during the time of the release was almost due west, which allowed the vertical configuration to capture the plume from the tracer release. The soaker hoses were set up in an "H" configuration to simulate an area source, and the approximate dimensions of the "H" configuration were 10 meters wide and 40 meters long on each side. Using a digital scale, the weight of the ethylene cylinder was recorded prior to release of the gas and immediately after the release was completed. In addition, the precise starting and ending time of the release was recorded in order to calculate the average actual flux of ethylene. This flux value was then compared to the ethylene flux calculated from the vertical scanning survey.

Figure 4-1 shows a schematic of the vertical scanning configuration used to simultaneously measure the methane emissions and the ethylene tracer plume. The configuration is overlaid by

the ethylene plume profile in the form of concentration contours as determined by the RPM algorithm. The emission flux through the vertical measurement plane, calculated from the area integration of the concentration profile multiplied by the component of the wind speed normal to the vertical plane, was determined as 0.98 g/sec. Since the measurement plane captured the entire plume, the entire flux through the plane is the emission rate of ethylene.

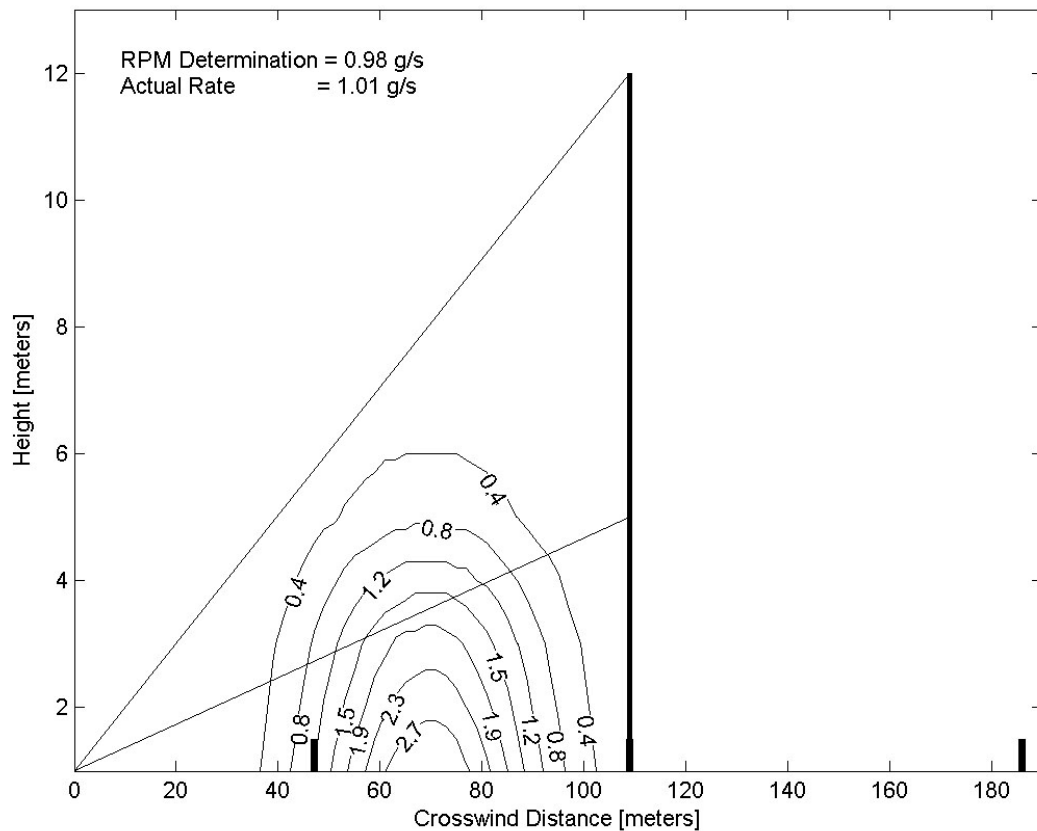


Figure 4-1. OP-FTIR RPM Measurement of the Vertical Ethylene Tracer Plume Profile on the Western (Upwind) Side of the Landfill. These Determinations Were Made from the Same OP-FTIR Measurements as the Methane Vertical Plume Profile (numbers on the isopleths are the ethylene concentrations in ppm).

Ethylene tracer gas was released for 75 minutes. During this period, the measured mass of the ethylene cylinder was reduced by 4.59 kg. A loss of 4.59 kg over a 75-minute period indicates an average flow rate of 1.02 g/sec. The measured emission rate indicates an ethylene mass recovery of 96%.

The flux of the ethylene release determined by mass-loss agrees well with the average ethylene flux calculated from the vertical scanning survey. Observed wind directions during the vertical scanning survey were not highly variable, which is indicative of a stable atmosphere. Hashmonay et al. [2001] found that fluxes calculated during stable environments underestimated the actual flux by around 12%. The average ethylene flux calculated during the current experiment underestimated the actual average ethylene flux by 3.9%.

The favorable results found were due to the orientation of the prevailing winds, with respect to the vertical configuration. Table 3-2 shows that the observed wind direction was generally perpendicular to the vertical configuration during the entire survey. This allowed the configuration to capture a large amount of the ethylene plume from the site. Another factor that contributed to the favorable results found was the small variability in wind direction and speed during the period of the survey, which indicates very stable atmospheric conditions. Flux calculations in unstable atmospheric conditions tend to underestimate down to 60% of the actual fluxes (Hashmonay et al., 2001).

Figure 4-2 shows a time series of the calculated ethylene fluxes measured during the tracer release study. It is apparent that the calculated flux decreases sharply with time. This was expected, as the ethylene flow rate was decreased rapidly after the experiment began in order to prevent the regulator on the cylinder from freezing. It is important to note that, despite the fluctuation in the actual flow rate of the ethylene release, the experiment still yielded very favorable results.

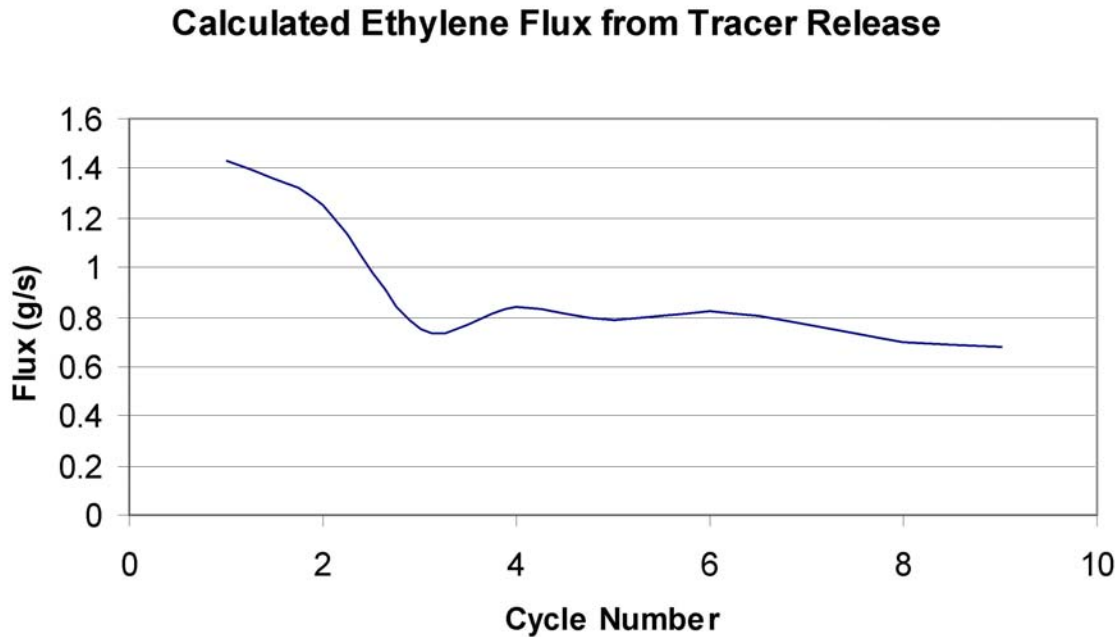


Figure 4-2. Time Series of the Calculated Ethylene Flux from Tracer Release Experiment

4.3 Assessment of Number of Cycles Used for Moving Average

A statistical analysis of the methane fluxes (measured from the vertical scanning configuration) was done to investigate trends in methane concentrations, standard deviations, and the average CCF when a different number of cycles is used for the moving average. The statistical analysis suggests that a moving average of four cycles is sufficient to provide a valid emission flux. Figure 4-3 shows the average methane flux and average CCF calculated using many different numbers of cycles for the moving average. The figure shows that the average calculated methane flux increases slightly as the number of cycles used for the moving average increases but begins to level off after two cycles. Additionally, the figure shows that the standard deviations of methane fluxes decreases after two cycles. The CCF plot shows a similar trend, with values leveling off after four cycles, and standard deviations decreasing as well.

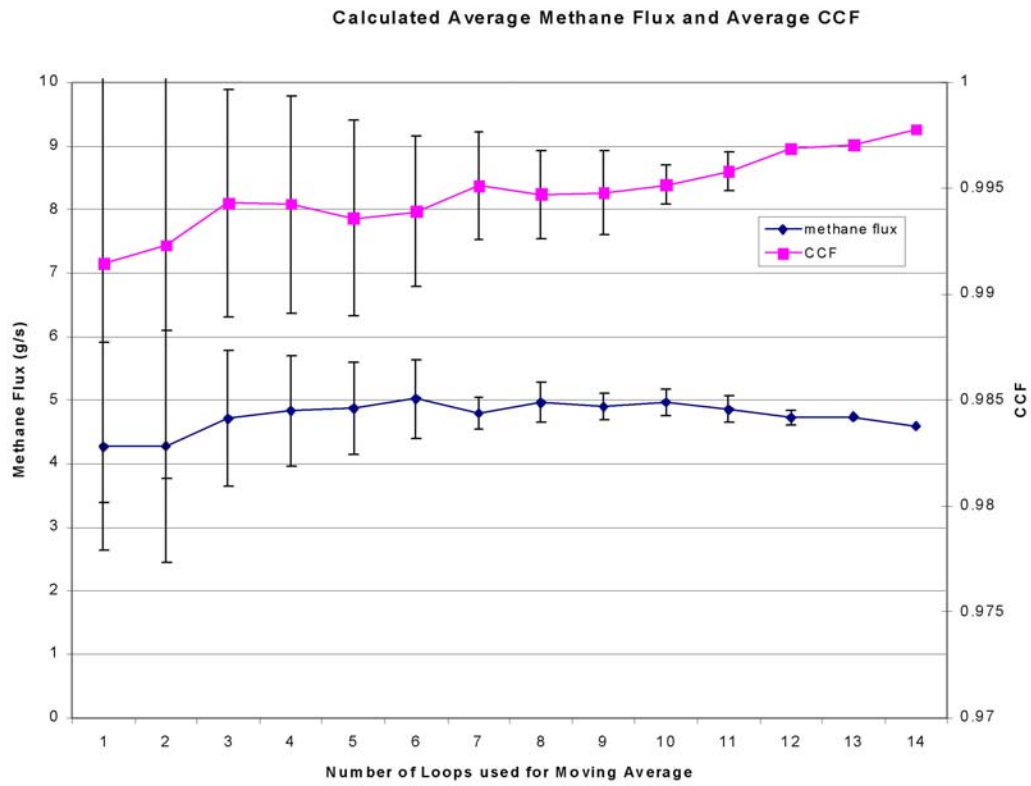


Figure 4-3. Calculated Average Methane Flux and Average CCF from the Vertical Scanning Survey

5.0

Conclusion

The present study employed Open-path FTIR sensors to determine chemical concentrations over the entire area of the Superfund landfill in Somersworth, New Hampshire. The spatial information was extracted from the path-integrated open-path FTIR measurements using the RPM method. This measurement-based technique provided a complete methane concentration-contour map of the entire landfill and located areas of high methane emissions (up to 6.5 ppm average methane concentration above the global background). In addition, the vertical scanning technique provided an estimate for the methane emission of 5.8 g/sec from the entire landfill. The methane emission rate from the hot spots in the valley was determined to be 3.3 g/sec, which is 57 percent of the emission from the entire landfill. The vertical scanning technique was tested for accuracy by using ethylene tracer release. The RPM determination of the ethylene emission rate agreed with the actual release rate to within four percent.

6.0

References

Hashmonay, R.A., K. Wagoner, D.F. Natschke, D.B. Harris, and E.L. Thompson, Radial Computed Tomography of Air Contaminants Using Optical Remote Sensing, presented at the AWMA 95th Annual Conference and Exhibition, Baltimore, MD, June 23-27, 2002.

Hashmonay, R.A., D.F. Natschke, K. Wagoner, D.B. Harris, E.L. Thompson, and M.G. Yost, Field Evaluation of a Method for Estimating Gaseous Fluxes from Area Sources Using Open-Path Fourier Transform Infrared, *Environ. Sci. Technol.*, **35**, 2309-2313, 2001.

Hashmonay, R.A., and M.G. Yost, Innovative Approach for Estimating Fugitive Gaseous Fluxes Using Computed Tomography and Remote Optical Sensing Techniques, *J. Air Waste Manage. Assoc.*, **49**, 966-972, 1999.

Hashmonay, R.A., M.G. Yost, D.B. Harris, and E.L. Thompson, Simulation Study for Gaseous Fluxes from an Area Source Using Computed Tomography and Optical Remote Sensing, presented at SPIE Conference on Environmental Monitoring and Remediation Technologies, Boston, MA, Nov., 1998, in SPIE Vol. **3534**, 405-410.

Hashmonay, R.A., M.G. Yost, and Chang-Fu Wu, Computed Tomography of Air Pollutants Using Radial Scanning Path-Integrated Optical Remote Sensing, *Atmospheric Environment*, **33** (2), 267-274, 1999.

Wu, C-F., M.G. Yost, R.A., Hashmonay, D.Y. Park, Experimental Evaluation of a Radial Beam Geometry for Mapping Air Pollutants Using Optical Remote Sensing and Computed Tomography, *Atmospheric Environment*, **33** (28), 4709-4716, 1999.

Tsai, M.Y., M.G. Yost, C.F. Wu, R.A. Hashmonay, and T.V. Larson, Line Profile Reconstruction: Validation and Comparison of Reconstruction Methods, *Atmospheric Environment*, **35** (28), 4791-4799, 2001.